Implementing Microfluidic Flow Device Model in Utilizing Dural Substitutes as Pulp Capping Materials for Vital Pulp Therapy

Yoon, Hi-Won

Department of Dentistry

Graduate School

Yonsei University

Implementing Microfluidic Flow Device Model in Utilizing Dural Substitutes as Pulp Capping Materials for Vital Pulp Therapy

Advisor Shin, Su-Jung

**A Master's Thesis Submitted
to the Department of Dentistry
and the Committee on Graduate School
of Yonsei University in Partial Fulfillment of the
Requirements for the Degree of
Master of Dental Science**

Yoon, Hi-Won

June 2025

Implementing Microfluidic Flow Device Model in Utilizing Dural Substitutes as Pulp Capping Materials for Vital Pulp Therapy

This Certifies that the Master's Thesis of Yoon, Hi-Won is Approved.

Committee Chair	**Kim, Sunil**
Committee Member	**Shin, Su-Jung**
Committee Member	**Kwon, Jae-Sung**

Department of Dentistry
Graduate School
Yonsei University
June 2025

감사의 글

지난 석사과정 2년과 본 학위논문을 무사히 마치기까지 지혜와 도움을 주신 많은 분들께 깊은 은혜를 입으며 감사의 말씀을 전하고자 합니다.

본 논문을 작성하며 부족한 저를 관심과 열정으로 지도해주신 신수정 교수님께 진심으로 감사드립니다. 깊이 존경하는 마음을 이 글을 통해 전하고 싶습니다. 또한 바쁘신 와중에도 논문 심사를 맡아 주시고 귀중한 조언과 통찰을 아끼지 않으신 김선일 교수님, 권재성 교수님께도 감사의 말씀을 올립니다.

보존과 수련 기간 동안 한결 같은 온기로 이끌어 주시고 가르쳐 주신 박정원 교수님께도 깊이 감사드립니다. 또한 보존과 수련의로서, 또 대학원생으로서 지식의 넓이와 깊이를 더할 수 있도록 아낌없는 가르침을 주신 김의성 교수님, 정일영 교수님, 신유석 교수님, 김도현 교수님께도 감사의 말씀을 드립니다.

함께 수련을 받으며 서로에게 힘이 되어주고, 즐거운 수련 생활을 할 수 있게 해준 동기 김윤희 선생님과 의국 선후배님들께도 감사의 말씀을 전합니다.

마지막으로 언제나 묵묵히 믿어 주시고 든든하게 저를 지지해주신 사랑하는 부모님께 깊은 감사를 전합니다. 멀리서도 응원해 준 언니와 오빠에게도 따뜻한 마음을 전합니다. 그리고 인생의 가장 큰 선물이자 든든한 동반자인 사랑하는 남편 민용, 언제나 웃음으로 하루를 밝혀주는 소중한 딸 율 에게 이 논문을 바치는 마음으로, 무한한 사랑과 감사의 마음을 담아 이 글을 마칩니다.

TABLE OF CONTENTS

LIST OF FIGURES

LIST OF TABLES

ABSTRACT

Implementing Microfluidic Flow Device Model in Utilizing Dural Substitutes as Pulp Capping Materials for Vital Pulp Therapy

Vital pulp therapy (VPT) has gained prominence with the increasing trends towards conservative dental treatment with specific indications for preserving tooth vitality by selectively removing the inflamed tissue instead of the entire dental pulp. Although VPT has shown high success rates in long-term follow-up, adverse effects have been reported due to the calcification of tooth canals by mineral trioxide aggregates (MTA), which are commonly used in VPT. Canal calcification poses challenges for accessing instruments during retreatment procedures. To address this issue, the present study investigates the potential of dural substitutes as alternative pulp capping materials with mechanical and biological properties favorable for maintaining pulp health while reducing canal calcification risk.

Specifically, the study assessed the mechanical characteristics of two dural substitutes, Biodesign (BD) and Neuro–patch (NP), designed to alleviate intra–pulpal pressure associated with inflammation. The biological responses of human dental pulp stem cells (hDPSC), which are essential for pulp regeneration and repair, were evaluated *in vitro*. A microfluidic flow device was developed to simulate the dynamic blood flow environment of the dental pulp, with computational fluid dynamics (CFD) simulations confirming that the device accurately reproduced physiological flow velocities.

In addition, the barrier properties of the dural substitutes were tested against 2–hydroxypropyl methacrylate (HEMA), a cytotoxic monomer released from bonding agents

and restorative materials. Both BD and NP demonstrated effective resistance to HEMA penetration, suggesting their potential to protect pulp tissue from chemical irritation. The biological responses observed in the microfluidic device closely paralleled those found in live pulp tissues, highlighting the utility of this platform as a physiologically relevant *in vitro* model for future VPT material testing.

These findings support the use of dural substitutes as promising alternatives to MTA in vital pulp therapy, offering both biological compatibility and protection from external irritants, while also presenting a novel microfluidic approach for *in vitro* pulp tissue modeling.

Key words: Dural substitute, Human dental pulp stem cell, Microfluidic flow device, Vital pulp therapy

I. INTRODUCTION

Vital pulp therapy (VPT) is considered an alternative to conventional endodontic treatment in specific cases, with the goal of removing inflamed pulpal tissue while preserving pulp vitality (Cohenca et al., 2013) (Dumbryte et al., 2021). According to a cohort study, the success rate of VPT was reported to be 91.6 % over a 10 years follow-up period (Asgary et al., 2024). The American Academy of Pediatric Dentistry encourages dentists to use VPT for immature permanent teeth. Mineral trioxide aggregate (MTA), composed of calcium silicate and calcium aluminate, is the most common pulp capping material used during VPT (Camilleri, 2008). However, MTA sometimes aggressively upregulates genes related to hard tissue formation, thereby potentially leading to intra-canal calcification (Boontankun et al., 2023). Intra-canal calcification poses a risk as it can obstruct access for instrument during endodontic treatment, with estimated prevalence ranging from 35 % to 91 % (Chen et al., 2012, Chueh et al., 2009).

The dental pulp and brain share common feature: both are soft tissue enclosed within hard tissue, resulting in low compliance conditions. In the brain, this environment can be fatal in cases of edema due to high intracranial pressure causing ischemia (Patel et al., 2023). To alleviate intracranial pressure in inflamed brain conditions, cranial bone resection is performed, following by the application of dural substitute to cover the brain, allowing the pressure to return to a normal state (Vakis et al., 2006). Similarly, in the case of dental pulp inflammation, cytokines such as substance P and prostaglandin E2 are secreted, initially increasing blood flow. However, due to the low compliance conditions, blood flow subsequently decreases, leading the necrosis (Kim and Dorscher 1989), During VPT, the inflamed dental pulp experience high intra-pulpal pressure. Applying a dural substitute in VPT could potentially relieve this pressure and promote healing.

In a previous *in vivo* study, researchers applied bioresorbable membranes within dental pulp, and after six weeks, these membranes maintained the vitality of the dental pulp while increasing the blood supply (Marsan et al., 2003). Histologically, a dentin-like wall was

observed beneath the membrane. The process of odontoblast like cells reaching the membrane and internalizing these structure was noted. Additionally, degradation of the bioresorbable was observed (Lee et al., 2012). These fibrous membrane mimic the structure of extracellular matrix, and facilitate cell attachment and migration (Sowmya et al., 2010). Fibrous membranes, dural substitutes, are frequently used to cover soft tissues in cranial surgeries, thereby reducing the risk of infection and promoting tissue recovery (Berjano et al., 1999). Commonly used dural substitutes such as Biodesign (BD) and Neuro-patch (NP), which are recognized for their biocompatibility (Elhakim et al., 2023), and can be applied in both cranial surgeries and VPT. Dural substitutes have the potential to replace conventional VPT materials such as MTA and mitigate the risk of intra-canal calcification (Marsan et al., 2003).

Human dental pulp stem cells (hDPSC) and endothelial cells are integral components of dental pulp. The dental pulp tissue is highly vascularized and contains dental pulp stem cells that can differentiate into various cell types in response to specific stimuli (Li et al., 2020). While many previous *in vivo* studies have been conducted without considering the fluid flow conditions, recent studies have shifted their focus towards microfluidic organ-on-a-chip systems. Which offer more physiologically relevant properties and overcome the limitations of traditional *in vitro* studies (Huang et al., 2023). Cell culture under flow conditions *in vitro* replicates mechanical stimulation, known as shear stress, and elicits a physiological response that closely mimics *in vivo* behavior (Koutsiaris et al., 2007). Additionally, the microfluidic flow device model aids in observing real-time cellular reactions to external stimuli, thereby facilitating an understanding of characteristics of these stimuli and the application of biomaterials (Franca et al., 2020). In this study, a microfluidic flow device was developed to mimic dental pulp chambers and serves as an evaluation tool for investigating the effects of VPT materials on hDPSC. Figure 1 illustrates the conversion of a conventionally treated tooth for VPT into the microfluidic flow device model, including the application of dural substitutes as pulp capping materials.

The objective of this research was to explore the possibility of using dural substitute as

a pulp cover materials in VPT. Additionally, two null hypotheses were tested. The fist null hypothesis suggested that it would not be possible to apply shear stress to cells in the microfluidic flow device. The second null hypothesis was that the penetration resistance to 2-hydroxypropyl methacrylate (HEMA) would not be lower in dural substitutes compared to MTA.

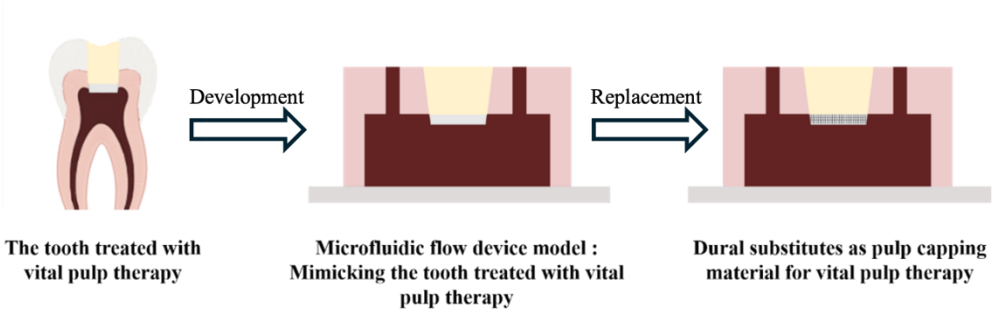

Figure 1. Schematic illustration of the microfluidic flow device system with various pulp capping materials

II. MATERIALS AND METHODS

Three independent experiments were replicated and using at least three replicates in each experiment, and data from those showing similar tendencies were included in the results section. The experimental materials and their detailed composition have been summarized in Table 1.

Table 1. Information of used materials.

Materials	Abbreviation	Manufacturer	Composition
ProRoot MTA	MTA	Dentsply Sirona, Tulsa, OK, USA	Bismuth oxide, tricalcium silicate, dicalcium silicate, calcium dealuminate, and calcium sulfate dehydrate
Biodesign Dural Graft	BD	Cook Biotech, West Lafayette, IN, USA	Collagen membrane sheet from decellularized small intestinal submucosa
Neuro-Patch	NP	B.Braun, Melsungen, Germany	Synthetic membrane sheet made of polyester urethane
Histoacryl	HA	B.Braun, Melsungen, Germany	N-butyl-2-cyanoacrylate

1. Part I. Preparation and characterization of microfluidic flow device

1.1 Fabrication of microfluidic flow device

The negative mold for the microfluidic flow device was designed using the Tinkercad software (Autodesk INC, San Rafael, CA, USA) and printed using a 3D printer (Nextdent 5100; 3D Systems, Rock Hill, SC, USA) with a resin slurry (Nextdent Ortho Rigid; 3D

System). The dimensions of the printed mold are presented in Figure 2(a). To remove any remaining monomer from the mold it was sonicated twice in isopropyl alcohol (Sigma-Aldrich, St Louis, MO, USA) for 15 min each time, and then post-cured for 1 h using a post-curing box (LD-3DPrint BOX, 3D Systems). Following this, the mold was heat treated at 100 ℃ for 2 h in electrical furnace (Venzac et al., 20). Polydimethylsiloxane (PDMS) and its catalyst were mixed at a ratio of 10:1 using a speed mixer (Hauschild, Hamm, Germany) at 3,500 rpm for 90 s, and 40 mL of the mixture was poured into a mold. Subsequently, it was degassed for 2 h at room temperature to remove embedded air bubbles. After completing this step, the mold was placed in a 50 ℃ furnace overnight (Figure 2(b)). The cured microfluidic flow device was removed from the mold, and a 10 × 10 mm^2 window was created in the center of the chip to place various materials such as MTA, BD, and NP. Following the manufacturer's instruction, mixed MTA was place in the window to a thickness of 1 mm. Additionally, BD and NP, each measuring 1.3 × 1.3 mm^2, were affixed onto the window using 0.015 g HA, which was evenly applied along the edge of the dural substitute in all subsequent experiments (Figure 2(c)). These were then stored in a cell incubation for 1 d. The microfluidic flow device and a 76 × 52 mm^2 slide glass were placed in an oxygen plasma treatment appliance (Zepto-modell2; Diener Plasma GmbH & Co., Ebhausen, Germany) for 4 min. After the treatment, the microfluidic flow device was attached to a glass slide using slight pressure, finally forming a completely sealed microfluidic flow device. Prior to cell culturing, microfluidic flow device was sterilized with 70 % ethanol for 10 min and washed thrice with photphate-buffered saline (Welgene, Gyeongsan, Gyeongsangbuk-do, Korea).

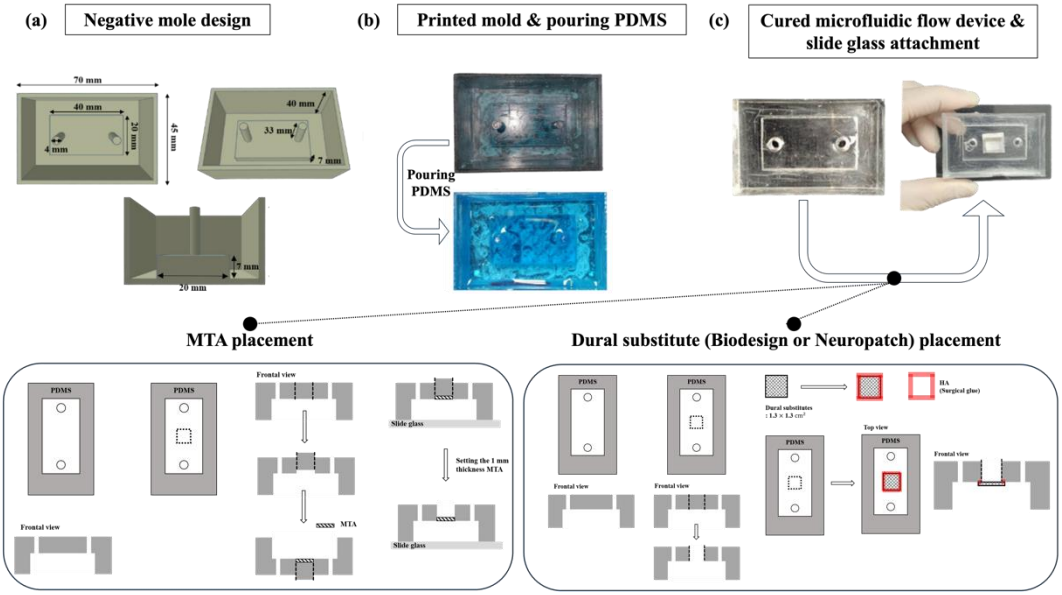

Figure 2. Fabrication protocol of the microfluidic flow device. (a) Dimensions of the negative mold of the microfluidic flow device. (b) Images illustrating the 3D printed negative mold of the microfluidic flow device and the pouring of polydimethylsiloxane (PDMS) into the mold. (c) After curing PDMS, removing the mold from cured PDMS chip and assembling slide glass while applying various pulp capping material. The completed microfluidic flow device is shown.

1.2 Analysis fluid flow dynamics within microfluidic flow device

After designing the microfluidic flow device model using Tinkercad software, it was employed for computational fluid dynamics (CFD) analysis (Autodesk INC) to assess the effects of fluid flow and shear stress on the bottom surface. Using the microfluidic flow device model (Figure 2(c)) as the basis, CFD was employed to simulate the isothermal fluid flow within the pulp. The fluid density was set as 1.0×10^6 kg/m^3, with an inlet fluid flow

velocity of 2.65 cm/s and an outlet pressure of 0 Pa. The flow velocity results across various planes were confirmed after 100 simulation cycles.

2. Part II. Cell culture and proliferation in the microfluidic flow device

2.1 Cell culture

For hDPSC (Lonza, Basel, Switzerland), alpha modified Eagle's medium (α-MEM; Welgene) supplemented with 10 % fetal bovine serum (FBS; Thermo Fisher Scientific, Waltham, MA, USA) and 1 % antibiotic-antimycotic (AA; Thermo Fisher Scientific) was used as culture medium. All cells used in this study were from passage 3-5 with seeding density of 1.0×10^5 were seeded onto a microfluidic flow device and incubated at 37 ℃ for 1 d. Subsequently, the microfluidic flow device was placed on a hot plate set to 37 ℃. Polytetrafluoroethylene tubes, along with 4 mm outer diameter polyvinylidene fluoride connector, were connected to the inlet and outlet holes of the microfluidic flow device. A perfusion pump (ISMATEC, Zurich, Switzerland) was used to flow the culture medium from the bottle filled with medium at 37 ℃ into the system at a flow rate of 0.3 mL/min and the effluent medium was collected in another bottle. Medium was removed after 1 d and replaced with fresh medium. The process was repeated for 7 or 14 d.

2.2 Evaluation of cell attachment and growth across different region

hDPSC were cultured for 7 d under flow conditions described in section 2.1. Cell attachment and growth were then observed using microscope at 10 × magnification across different regions of the microfluidic flow device. As shown in Figure 3, five different sites were chosen to evaluated the effect of fluid flow, shear stress, and pulp capping materials on cell behavior. Observation sites for evaluating cell attachment and growth within the microfluidic flow device in the presence of pulp capping materials

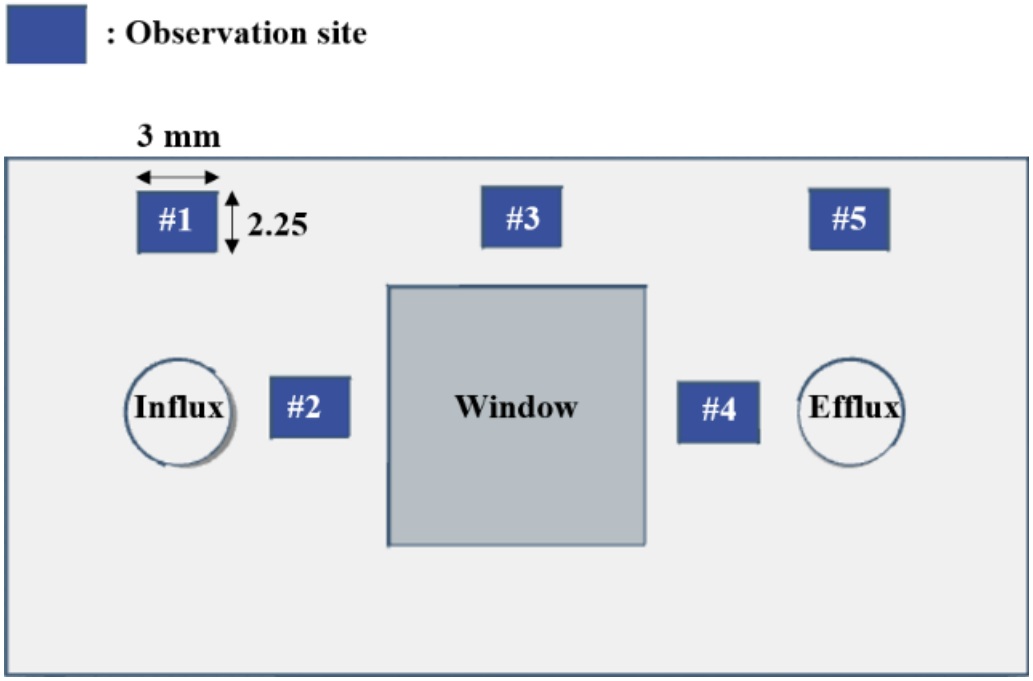

Figure 3. Observation sites for evaluating cell attachment and growth within the microfluidic flow device in the presence of pulp capping materials. These figure exhibits the dimension of the inner space of the microfluidic flow device.

3. Part III. Physical and chemical evaluation of pulp capping materials

3.1 Physical characteristics of dural substitutes

Tensile stress tests were conducted using a universal testing machine (Instron 5942; Instron, Norwood, MA, USA) with crosshead speed of 1 mm/min. Specimens of BD and NP were cut into dumbbell bell shape and the thickness of each dural substitute was measured using a digital caliper (Mitutoyo Kawasaki, Kanagawa, Japan), confirming a thickness of 0.15 mm (Figure 4(a) and 4(b)). For the membrane bulging test, each dural

substitute was cut into a circular shape with a 5 mm diameter and attached to a substrate with a 4 mm diameter space using histoacryl (HA), ensuring a wrinkle-free and tension free state. A pressure of 20 g was applied using a 2 mm diameter hemispherical cylinder at the center of attached dural substitute, and the stretched ehight of the dural substitute was measured using a magnifying camera (SmartDrop Lite; Femtobiomed, Seongnam, Gyeonggi-do, Korea) (Figure 4(c)). Each tensile and bulging test was performed in triplicates for both dural substitutes.

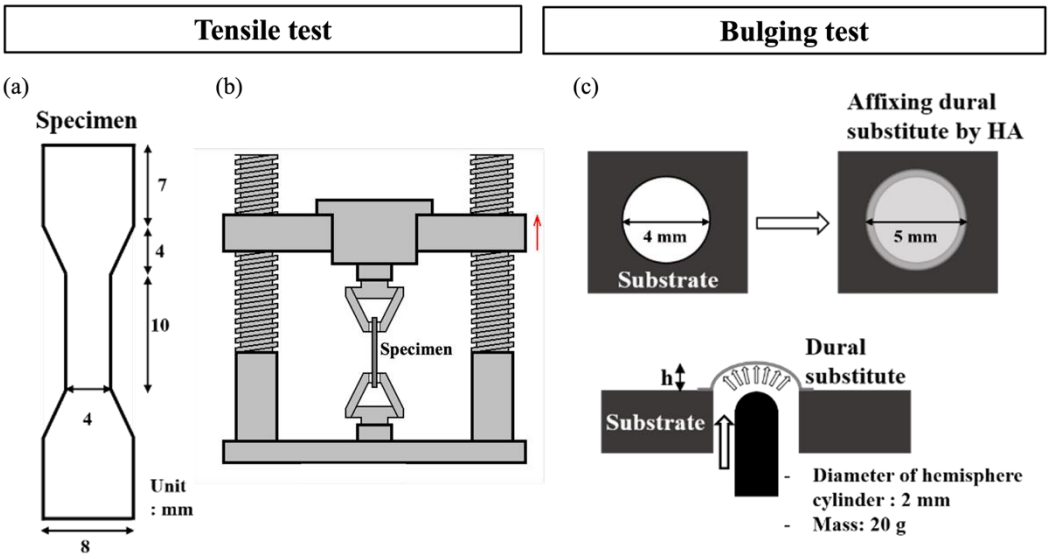

Figure 4. Schematics diagrams of tensile and bulging test protocol. (a) Dimension of dural substitute specimen for tensile stress test. (b) Test method of tensile test by using universal testing machine. (c) Protocol for the membrane bulging test and specimen dimension.

3.2 Wettability test

A static contact angle analyzer (SmartDrop Lite; Femtobiomed) was used to analyze the wettability of different pulp capping materials. A 5 μL droplet of HEMA solution was dispensed onto each materials using a needle tip. The resulting contact angle on each

sample's surface was measured and recorded 5 s after the droplet was dispensed. For each pulp capping material, the contact angle measurement was repeated six times and this process was conducted in triplicate.

3.3 Evaluation of kinetic permeation of pulp capping materials

The kinetic permeation of pulp capping materials was measured using the MINUSHEET perfusion system (Minucells and Minutissue, Bad Abbach, Germany). First, a 1 mm thicker layer of MTA or 0.15 mm thickness BD and NP was placed on the base part of the tissue carrier, and the pulp capping material was mounted on the base part. Next, the upper part ring was inserted into the base part groove to affix pulp capping materials. The assembled tissue carrier was then placed on the MINUSHEET perfusion culture system (Figure 5(a)). A volume of 500 μL of Rhodamine B (RhB; Sigma-Aldrich) was dropped on top of the pulp capping material and left for 3 h. The perfusion rate was set at 15 μL/min, and the perfused solution was collected every 10 min in 96 well plate. RhB has a maximum absorbance at 570 nm wavelength. The concentration of RhB was measured using a microplate reader (BioTek, Winnooski VT, USA) in triplicate for each capping materials (Figure 5(b)).

3.4 Penetration resistance to HEMA in accordance with materials

The microfluidic flow device containing hDPSC, which had been incubated for 7 d under flow conditions, was placed and secured onto an automated fluorescence microscope (EVOS FL; Thermo Fisher Scientific) diluted in medium to detect dead cell. The volume of 2.5 μM SYTO-9 (Thermo Fisher Scientific) diluted in medium to detect dead cell. The volume of 2.5 μM SYTO-9 used was 4 mL. Subsequently, 3 mL of solution of 20 mM HEMA solution was applied to the microfluidic flow device window, allowing HEMA to penetrate the MTA, BD, and NP. Bright-field and red-fluorescence images (indicative of dead cells) were captured every 10 min at room temperature. Positive control was used to

facilitate comparisons among the three experimental groups. For each group, the time at which half of the cells died was monitored (Figure 5(c)).

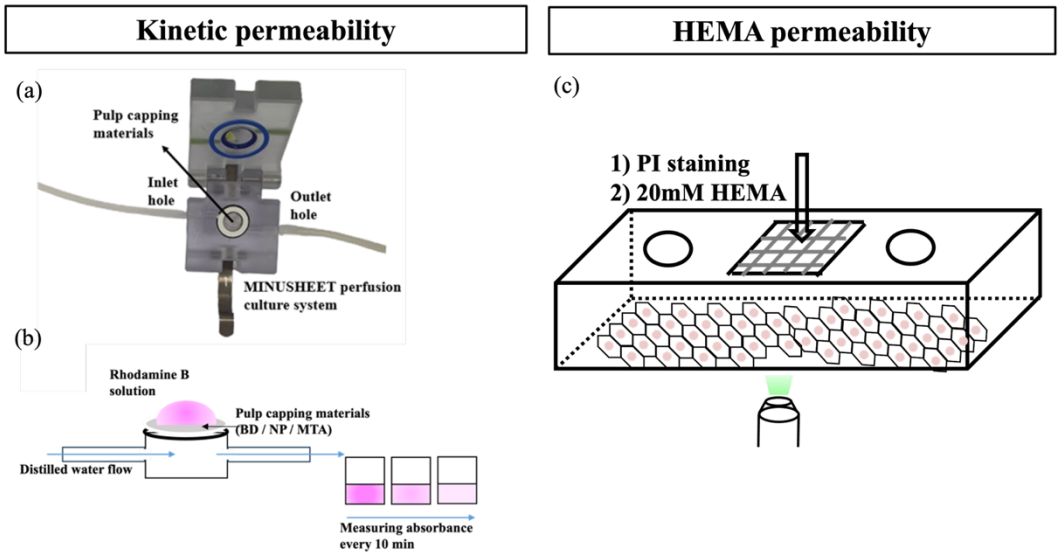

Figure 5. Kinetic permation and HEMA permeation analysis of tested pulp capping materials. (a) Experimental setup of kinetic permeation analysis. (b) Schematic figure to explain experiment process. (c) Real-time cytotoxicity evaluation by using PI staining.

3.5 Statistical analysis

One-way ANOVA followed by Tukey's test was utilized under the assumption of homogeneity of variance, whereas the Kruskal Wallis test followed by Dunn's test was employed under the assumption of non-homogeneity of variance. All statistical analyses were performed using SPSS software (version 27.0; IBM, Armonk, NY, USA). The significance level was set at $p<0.05$.

III. RESULTS

1. Part I. Preparation and characterization of microfluidic flow device

1.1 Fluidic flow analysis under CFD simulation

The fluid flow velocity within the microfluidic flow device, mimicking the pulp chamber, was simulated and analyzed, as shown in Figure 6(a). The fluid flow velocity within the microfluidic flow device, mimicking the pulp chamber, was simulated and analyzed, as shown in Figure 6(b)-(d), based on different planes relative to the x-, y-, and z-axes. Additionally, the shear stress on the bottom surface perpendicular to z-axis, is represented in Figure 6(e). The influx fluid moved downward and rotated when it reached the bottom surface, similarly, the fluid at the middle plane circulated in both upward and downwards direction. While the efflux fluid moved upward at slower rate compared to the influx fluid (Figure 6(b) and (c)). Furthermore, the influx fluid initially spread radially on the bottom surface of the microfluidic flow device and then flowed in the y-axis direction until it originated from the efflux hole. The fluid flow velocity at the bottom side of the microfluidic flow device ranged from 0.265 cm/s to 1.37 cm/s. Moreover, the shear stress at the bottom of the microfluidic flow device ranged from 0.02 dyne/cm^2 to 0.15 dyne/cm^2 in Figure 6(e). Considering that cells attached the bottom surface, this microfluidic device can apply shear stress to cells and mimic the physiological conditions of the dental pulp, such as fluid flow and shear stress.

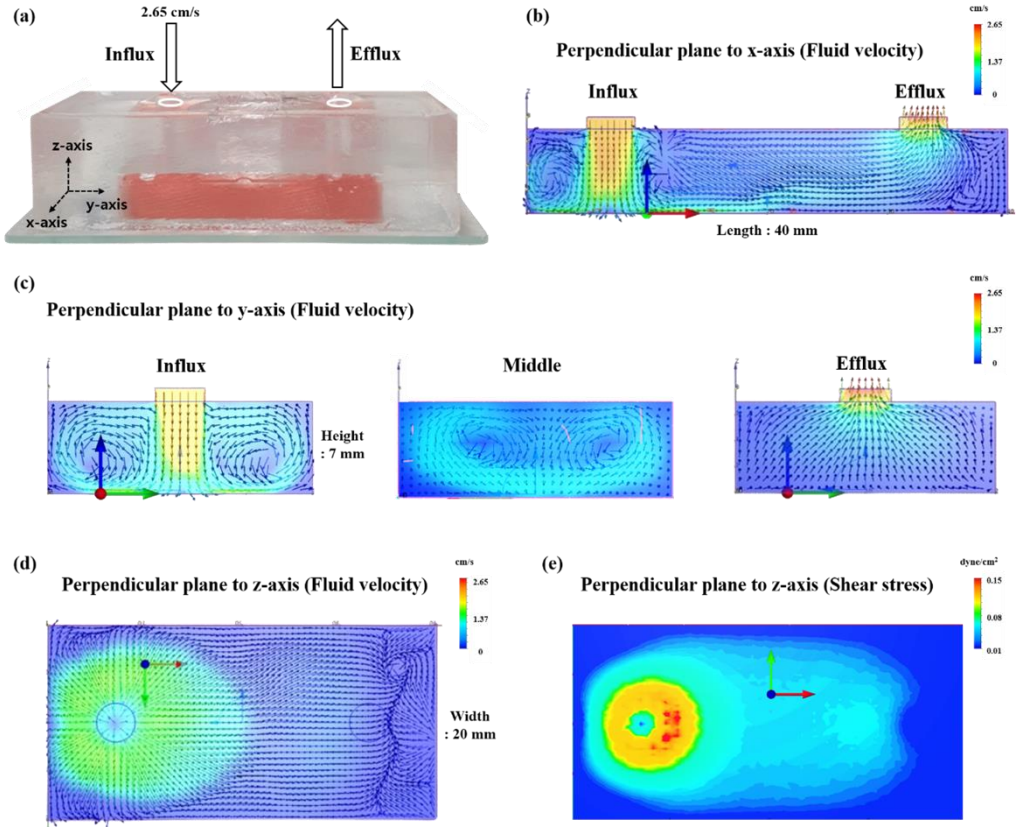

Figure 6. Analysis of fluid flow velocity in the microfluidic flow device model across various surfaces using computational dynamics simulation: (a) Detailed fluid flow conditions and x, y, and z axes of the microfluidic flow device. (b) Fluid simulation analysis of the central perpendicular plane to x-axis. (c) Fluid simulation analysis of perpendicular plane to the y-axis at the influx hole (left), center (middle), and efflux hole (right). (d) Fluid simulation analysis of the perpendicular plane to the z-axis at the bottom of the microfluidic flow device. (e) Shear stress analysis in the plane perpendicular to the z-axis at the bottom of the microfluidic flow device.

2. Part II. Cell culture and proliferation in the microfluidic flow device

2.1 Evaluation cell attachment and growth across different region within microfluidic flow device

Figure 7 depict hDPSC cultured for 7 d under flow conditions within a microfluidic flow device. Each cell type was exposed to various pulp capping material and shear stress, with hDPSC observed at sites labeled from #1 to #5 sites in Figure 7. Generally, cells in site #1 and #2 exhibited lower confluence compared to sites #3, #4, and #5. Upon considering the morphology of cells across different sites, applied shear stress ranging from 0.02 dyne/cm^2 to 0.15 dyne/cm^2 did not significantly alter cell morphology. Consequently, the designed microfluidic flow device ensured uniform distribution and attachment of cells across all surfaces where cell adhered.

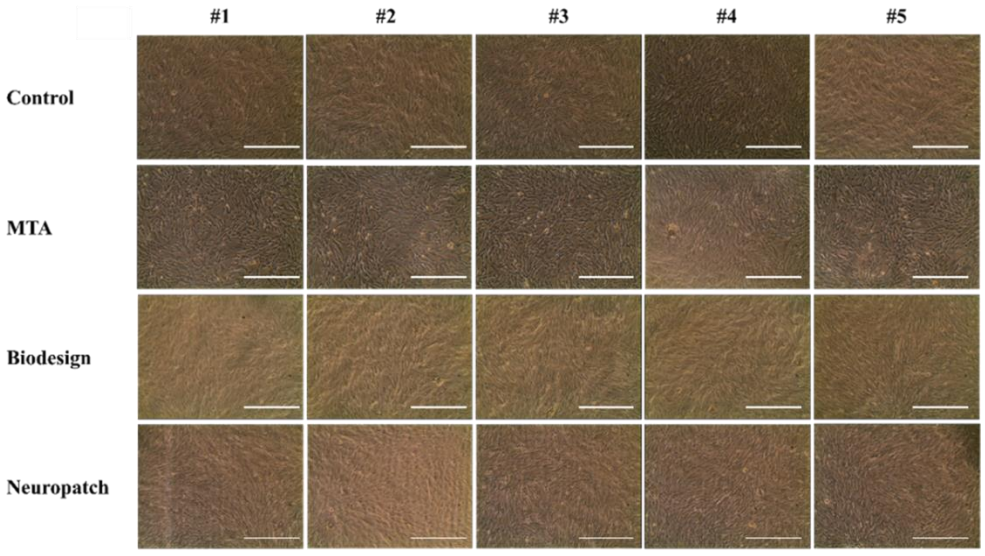

Figure 7. Images of hDPSC and HUVEC cultured for 7 d within a microfluidic flow device across different sites. hDPSC cultured in microfluidic flow device with different pulp

capping materials for 7 d. Each images measures 3 × 2.25 mm^2 at a magnification of ×10. (Scale bar: 200 μm).

3. Part III. Physical and chemical evaluation of pulp capping materials

3.1 Tensile stress and membrane bulging test

As shown in Figure 8(a) and 8(b), the elastic modulus of BD was 5.82 ± 1.29 MPa, while that of NP was 0.071 ± 0.024 MPa. The ultimate tensile strength of BD was 17.02 ± 2.31 MPa, and for NP, it was 9.68 ± 1.66 MPa. The strain (%) values differed significantly between the two dural substitutes. BD exhibited low stretchability, with a strain value of approximately 5 %, whereas NP demonstrated high stretchability, with a strain value of around 180 %. Figure 8(a) and 8(b) illustrates that the stretched height (h) of BD was 0.089 ± 0.011 mm, while NP was 1.02 ± 0.08 mm. Consistent with the tensile stress test results, NP exhibited greater pliability when subjected to applied pressure.

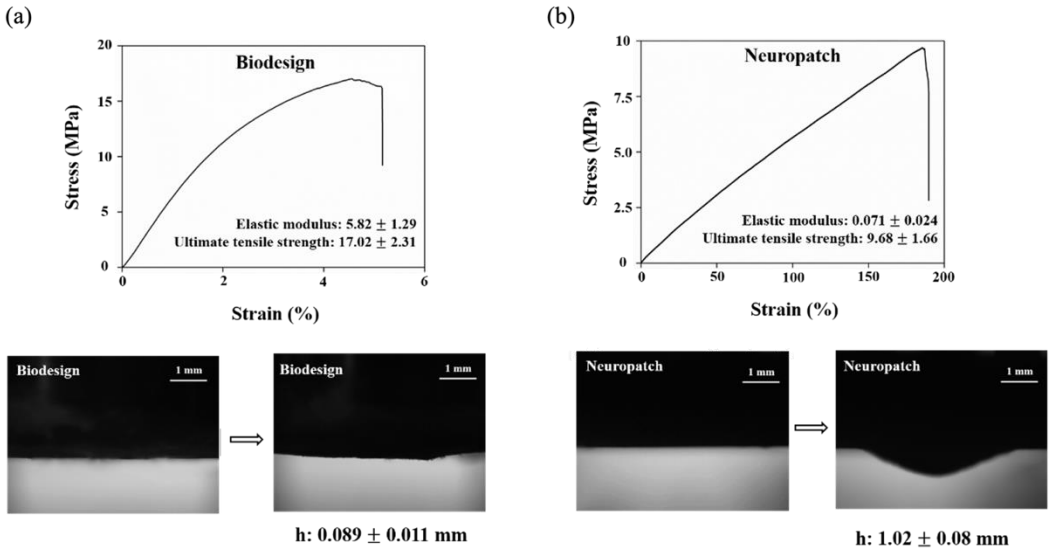

Figure 8. Results of tensile stress and membrane bulging test with specimen dimensions. (a) Results of stress-strain curve and bulging test of Biodesign. (b) Results of stress-strain curve and bulging test of Neuropatch.

3.2 Penetration resistance of pulp capping materials over time

The permeation of RhB solution varied over time depending on the pulp capping materials used in Figure 9. Correspondingly, the pulp capping materials demonstrated varying degrees of penetration resistance. In the case of MTA, the absorbance graph exhibited a steady increase from 30 min to 80 min, reaching a plateau that persisted until 180 min. Conversely, the graphs representing BD and NP displayed distinct patterns compared to MTA. Specifically, these dural substitutes exhibited a peak before 50 min, followed by a consistent decrease until 180 min. Notably, the absorbance of BD began to increase earlier than that of NP; at 20 min, the absorbance of BD reached 0.1, whereas NP at 0.04. Furthermore, the peak absorbance of BD occurred earlier than that of NP, Consequently, MTA demonstrated the highest resistance to penetration among the tested pulp capping materials, with NP exhibiting slightly superior resistance compared to BD.

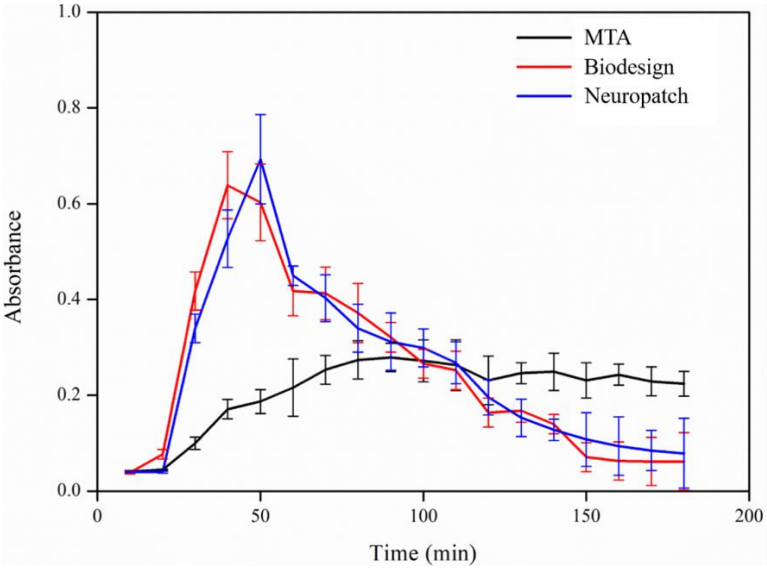

Figure 9. Kinetic permation analysis of tested pulp capping materials. The graph illustrates the absorbance of the RhB solution that permeated from the tested pulp capping materials, collected at 10 min intervals from 10 min to 180 min.

3.3 Wettability of different materials

In Table 2, the MTA group exhibited a contact angle of 7.983 ± 3.311 ° with 20 mm HEMA, while the BD group showed 65.114 ± 9.150 °, and NP group showed 109.18 ± 2.365 °. The order of wettability was MTA > BD > NP.

Table 2. Contact angle analysis.

Pulp capping materials	Contact angle of HEMA (°)
Mineral trioxide aggregate (MTA)	7.983 ± 3.311
Biodesign (BD)	65.114 ± 9.150
Neuropatch (NP)	109.18 ± 2.365

3.4 Evaluating the cytotoxicity of hDPSC upon exposure to HEMA

In Figure 10(a), the Positive control group, which was directly exposed to HEMA, exhibited over 50 % cell death between from 40 to 50 min. Additionally, among experimental groups such as MTA, BD, and NP, time to reach 50 % cell death was from 120 to 140 min, from 50 to 60 min, and from 80 to 90 min, respectively. These results indicate that MTA was the most efficient in resisting HEMA penetration among the pulp capping materials, followed by NP and BD (Figure 10(b)).

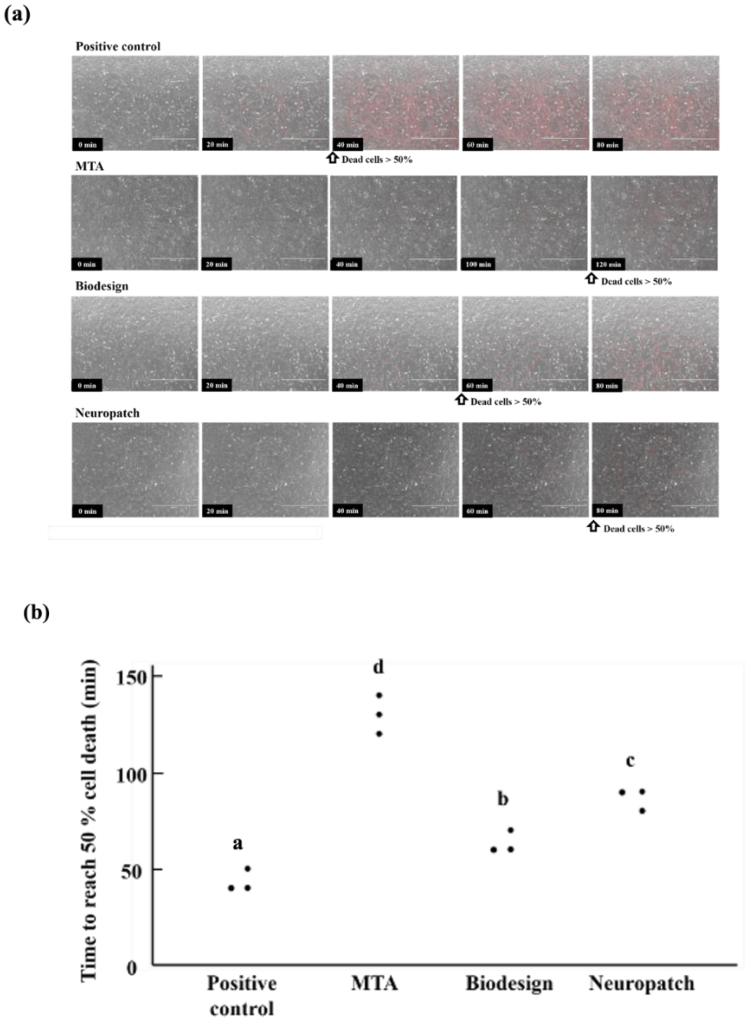

Figure 10. Real-time microscopy observation of hDPSC with HEMA. (a) Real-time microscopy observation of hDPSC with 20 mM HEMA and SYTO-9. Images were captured every 10 min. At 10 × magnification, bright-field images were overlaid with SYTO-9 signal (red). Point of exceeding 50 % cell death was assessed thrice for each group. (b) Time taken to reach 50 % cell death among groups, marked as dot on the graph. If the same time was recorded, these two points were marked horizontally. Different alphabets indicate a statistical difference between the groups ($p<0.05$). (Scale bar: 200 μm)

IV. DISCUSSION

MTA is considered the golden standard material in VPT protocol due to its ability to induce tertiary dentin formation (Kang et al., 2017). hDPSC have high differentiation and prolifereation into odontogenic cells that participate in tertiary dentin formation (Luke et al., 2020). Thus, hDPSC help maintain homeostasis in the dental pulp against external stimuli. However, the formation of tertiary dentin is not always beneficial for the dental pulp in terms of healing capability. As tertiary dentin formation progresses, the size of the pulp chamber is reduced, which can lead to decreased blood supply (Rowe and Pitt Ford 1990). This phenomenon implies that when reparative dentin is produced in the dental pulp, the collagenous portion increases while the cellular content decreases. Consequently, dental pulp that has experienced stimuli or aged pulp may have a diminished protective ability against future irritants (Seltzer et al., 1963). Therefore, there is a need for pulp capping materials that do not induce excess calcification of the pulp after VPT.

This study represents an initial exploration of the response of hDPSC to a dural substitute utilized as a pulp capping material within a microfluidic flow system. In addition to conventional *in vitro* testing, the microfluidic flow device model emulates the pulp chamber in a tooth and recreates a fluid-flow environment similar to that of an *in vivo* test. In a healthy human anterior maxillary tooth, the average blood flow rate of the pulp was approximately 0.5 cm/s ranging from 0.1 to 2.0 cm/s, as evaluated by Doppler flowmetry (Cho and Park, 2015). This study demonstrated that the fluid flow rate at the bottom of the microfluidic flow device ranged from 0.265 to 1.37 cm/s in Figure 6(d). Therefore, we speculate that the design and fluid flow operational conditions of the microfluidic flow device successfully mimicked the real pulp fluid flow environment in a tooth. Shear stress resulting from fluid flow can induce friction against the attached cells, thereby exerting mechanical stress that influences cytokine pathways and gene expression (LaMack and Friedman, 2007). As shown in Figure 6(e), the microfluidic flow device capable of applying

shear stress ranging from 0.02 to 0.15 dyne/cm^2. Although the actual shear stress of human capillaries has been reported 3 to 90 dyne/cm^2 (Koutsiaris et al., 2007), interstitial fluid does not produce as much shear stress as blood flow. Mesenchymal stem cells are typically exposed to shear stress ranging from 0.01 to 0.1 dyne/cm^2 (Kim et al., 2014) (Rutkowski and Swartz, 2007); therefore, the shear stress of 0.02 to 0.15 dyne/cm^2 generated by the microfluidic flow device is similar to *in vivo* conditions.

In contrast to other organs, the dental pulp consists of a complex vaascular network that produces microcirculation, resulting in non-unidirectional blood flow macroscopically (Kim. 1985) (Franca et al., 2019). Additionally, arteriovenous anastomoses are common in dental pulp vascular networks, causing turbulent flow in the vessels microscopically (Li et al., 2008). Due to the design of the microfluidic flow device shown in Figure 6(a), turbulent and circulated flow was produced in the inner space, affecting hDPSC (Figure 6(b)-(d)). As I focused on dental pulp physiology, it was necessary to examine the influence of pulp capping materials on hDPSC. If turbulent or circulatory flow did not occurred, extracts from pulp capping materials such as MTA, BD, and NP would have difficulty reaching the cells attached to the bottom surface. In previous research on tooth-on-a-chip (Hu et al., 2022), the fluid flow played a role in washing out toxic substance and supplying nutrient for cells. However, due to the unidirectional flow, only cells attached near the outlet hole were influenced by the tested materials, while cells attached from the inlet hole were not exposed to the extracts. In contrast, our microfluidic device could spread the influence of pulp capping materials not only to cells near the outlet hole but also to those near the inlet hole. Furthermore, other dental microfluidic devices, tooth-on-a-chip and pulp-dentin complex-on-a-chip (Franca et al., 2020) (Rodrigues et al., 2021), did not provide microfluidic conditions to cultured cells. Therefore, the design of our microfluidic device is novel and a suitable evaluating the response of hDPSC to pulp capping materials, mimicking dental pulp physiology. Additionally, hDPSC was cultured uniformly across the entire microfluidic flow device and did not show significantly different morphologies regarding spots within the device in Figure 7.

Dural substitutes are promising candidates for use as pulp capping materials. In skull radiographs of patients treated with cranial surgery and cover by dural substitutes, the substitutes allow for decompression by bulging outward (Kim et al., 2014). In normal monkey pulp, the pressure is approximately 15 mmHg. However, under inflamed conditions, pulp pressure increases to about 50 mmHg (Stenvik et al., 1972). Similarly, in human normal pulp, the pressure is 10 mmHg, but in inflamed pulp, it reaches 34.5 mmHg (Bender, 2000). Teeth have a low compliance structure, and increasing intra-pulp pressure can lead to necrosis (Heyeraas and Berggreen, 1999). If dural substitutes such as BD and NP are applied as pulp capping materials, they may alleviate the intra-pulp pressure. In Figure 8, both BD and NP were stretchable, but NP exhibited greater stretchability than BD due to differences in their composition. The bulging test demonstrated the potential of each dural substitute to relieve intra-pulp pressure by bulging outward. The width of the pulp in mandibular moral teeth has been reported to be 3.32 ± 0.49 mm (Ilguy et al., 2004); therefore, the diameter of the substrate for the bulging test was set at 4 mm. Additionally, considering the 20 g mass and dimensions of the hemispherical cylinder, the applied pressure exceeded 50 mmHg. Although applying a smaller pressure would have been stretched height under such conditions. Therefore, mass was increased and chose a 2 mm diameter hemisphere dimension to provide uniform pressure across the entire surface of the dural substitutes. However, when applying smaller pressure than this option, stretched value cannot be evaluated precisely.

To analyze the accurate kinetic penetration resistance of various pulp capping materials, the MINUSHEET perfusion system was utilized instead of the microfluidic flow device (Figure 9). Unlike the microfluidic flow device, which experienced turbulence and circulation, the MINUSHEET perfusion system operated with simple fluid input and output, eliminating inaccuracies in substance collection. The volume of collected permeated RhB solution was verified to match among groups. The findings form Figure 9 is supplemented in Figure 10(a). The time required to reach 50 % cell death was ordered as follows: BD, NP, and lastly MTA in Figure 10(b). Figure 9 indicates that among pulp capping materials,

MTA significantly prevents substance permeation compared to the dural substitute Also, the penetration of NP is slower than that of BD. Moreover, the contact angle of MTA with 20 mM HEMA was approximately 7.893 °, which indicates a potential disadvantage in terms of HEMA penetration despite its greater thickness. Conversely, NP which exhibited a higher contact angle than BD, is evidence that NP has a higher resistance to 20 mM HEMA penetration (Table 2).

During VPT in a tooth, resin application typically involves the placement of pulp capping materials. A bonding agent is applied prior to resin application, wherein HEMA serves as a necessary component to enhance the infiltration of the bonding agent into the dentin, thereby increasing the bonding strength (Nakabayashi and Takarada, 2002). However, HEMA binds to glutathione cysteine and interferes with cellular metabolism, particularly radical elimination (Circu and Aw, 2012). Previous research has indicated that the concentration of HEMA causing 50 % cell death is 7.5 mm (Lee et al., 2009), and composite resin can release HEMA towards the pulp via pulp capping materials (Reichl et al., 2012). Therefore, 20 mM HEMA was considered appropriate for evaluating cell cytotoxicity. In Figure 10(b), exposure to 20 mM HEMA induced 50 % cell death after 40 min. The MTA group exhibits a porous structure with surface pore sizes typically under 10 μm (Lee et al., 2024), and the thickness of the set MTA in the microfluidic flow device was 1 mm. However, BD and NP are porous membrane with surface pore sizes of approximately 10 μm, while their thickness was lower than that of MTA, at about 0.15 mm. When fixing the dural substitute in the microfluidic flow device, HA was only applied to the edges and a 20 mM HEMA solution was dropped at the center. This difference in thickness could affect the time required to reach 50 % cell death among pulp capping materials. BD is composed of collagen, whereas NP is composed of polyurethane. This difference in the materials can affect the contact angle of 20 mM HEMA, as shown in Table 2. The 1 mm thickness of MTA used in the experiments was more than five times thicker than BD and NP; however, the time required to reach 50 % cell death did not scale

proportionally. Moreover, although the difference in thickness between BD and NP was minimal, the time required to reach 50 % cell death varied.

In summary, this study explored the feasibility of using a dural substitute to replace MTA as a pulp capping material in VPT by utilizing the microfluidic flow device model. The application of the surgical glue HA facilitated easy placement and fixation of the dural substitute while preventing HEMA penetration, thus, maintaining biocompatibility of the pulp cell. However, this study also encountered several limitations. Firstly, the stress relief of dural substitutes in conditions mimicking real inflamed tissue was not observed in the microfluidic flow device. Instead, only a membrane bulging out test was performed by applying pressure. Secondly, the fluid flow in the microfluidic flow device model did not precisely replicate blood flow in the pulpal capillary vessels of a tooth and uniform shear stress was not applied across the microfluidic flow device. Additionally, these design limitations led to zones with extremely low flow and shear stress. In the future, the microfluidic flow device design would need to be revised to overcome these limitations and more accurately mimic the physiological conditions of pulpal blood flow and shear stress distribution. Thirdly, designed microfluidic flow device does not accurately reflect the actual pulp chamber. In our device, the holes for influx and efflux of fluid were placed on the same surface as the pulp capping materials. However, in a tooth blood flow originated and terminates at the apex, while pulp capping materials are placed in the coronal space (opposite surface). Further research addressing these limitations could enhance the understating and application of the microfluidic flow device model in dental research.

V. CONCLUSION

1. The fluidic flow velocity and shear stress at the bottom surface of the microfluidic flow device ranged from 0.265 to 1. 37 cm/s and 0.02 dyne/cm^2 to 0.15 dyne/cm^2, respectively. Based on these findings, the first null hypothesis was rejected

2. Among the experimental groups - MTA, BD, and NP- the time to reach 50 % cell death ranged from 120 - 140 min, 50 - 60 min, and 80-90 min, respectively. Accordingly, the second null hypothesis was also rejected.

3. The microfluidic flow device model provides a valuable platform for studying the effects of fluidic flow on cells, thereby effectively mimicking pulp physiology.

4. Dural substitutes, specifically BD and NP, exhibited resistance to HEMA exposure.

5. Dural substitutes demonstrated promising biocompatibility as pulp capping materials and may help prevent unintended intracanal calcification.

References

Boontankun A, Manmontri C, Chaipattanawan N, Chompu-inwai P (2023). Pulp canal calcification in young permanent teeth that have undergone vital pulp therapy: a review. *Pediatric Dental Journa*l 33(3): 199–210.

Camilleri J (2008). The chemical composition of mineral trioxide aggregate. *Journal of Conservative Dentistry and Endodontics* 11(4): 141–143.

Chen M Y, Chen K L, Chen C A, Tayebaty F, Rosenberg P A, Lin L M (2012). Responses of immature permanent teeth with infected necrotic pulp tissue and apical periodontitis/abscess to revascularization procedures. *International Endodontic Journal* 4(3): 294–305.

Circu M L, Aw T Y (2012). Glutathione and modulation of cell apoptosis. *Biochimica et Biophysica Acta (BBA) – Molecular Cell Research* 1823(10): 1767–1777.

Cho Y W, Park S H (2015). Measurement of pulp blood flow rates in maxillary anterior teeth using ultrasound doppler flowmetry. *International Endodontic Journal* 48(12): 1175–1180.

Chueh L H, Ho Y C, Kuo T C, Lai W H, Chen Y H, Chiang C P (2009). Regenerative endodontic treatment for necrotic immature permanent teeth. *Journal of Endodontics* 35(2): 160–164.

Cohenca N, Paranjpe A, Berg J (2013). Vital pulp therapy. *Dental Clinics of North America* 57(1): 59–73.

Elhakim A, Kim S, Shin S J (2023). In vitro response of dental pulp stem cells to dural substitute grafts: analysis of cytocompatibility and bioactivity. *Internationial Endodontic Journal* 56(11): 1350–1359.

França C M, Tahayeri A, Rodrigues N S, Ferdosian S, Rontani R M P, Sereda G, et al. (2020). The tooth on-a-chip: a microphysiologic model system mimicking the biologic interface of the tooth with biomaterials. *Lab on a Chip* 20(2): 405–413.

Heyeraas K, Berggreen E (1999). Interstitial fluid pressure in normal and inflamed pulp. *Critical Reviews in Oral Biololgy and Medicine* 10(3): 328–336.

Hu S, Muniraj G, Mishra A, Hong K, Lum J L, Hong C H L, et al. (2022). Characterization of silver diamine fluoride cytotoxicity using microfluidic tooth on-a-chip and gingival equivalents. *Dental Materials* 38(8): 1385–1394.

Huang C, Sanaei F, Verdurmen W P R, Yang F, Ji W, Walboomers X F (2023). The application of oragns-on-a-chip in dental, oral, and craniofacial research. *Journal of Dental Research* 102(4): 364–375.

Ilguy D, Ilguy M, Bayirli G (2004). The size of dental pulp chamber in adult diabetic patients. *Oral Health Dental Management in the Black Sea Countries* 3(3): 38–41.

Kang C-M, Sun Y, Song J S, Pang N-S, Roh B-D, Lee C-Y, et al. (2017) A randomized controlled trial of various MTA materials for partial pulpotomy in permanent teeth. *Journal of Dentistry* 60: 8–13

Kim D-R, Yang S-H, Sung J-H, Lee S-W, Son B-C (2014). Significance of intracranial pressure monitoring after early decompressive craniectomy in patients with severe traumatic brain injury. *Journal of Korean Neurosurgical Society* 55(1): 26-31

Kim K M, Choi Y J, Hwang J-H, Kim A R, Cho H J, Hwang E S, et al. (2014) Shear stress induced by an interstitial level of slow flow increases the osteogenic differentiation of mesenchymal stem cells through TAZ activation. *PLoS One* 9(3): e92427

Kim S, Dörscher-Kim J (1989). Hemodynamic regulation of the dental pulp in a low compliance environment. *Journal of Endodontics* 15(9): 404–408.

Koutsiaris A G, Tachmitzi S V, Batis N, Kotoula M G, Karabatsas C H, Tsironi E, et al. (2007) Volume flow and wall shear stress quantification in the human conjunctival capillaries and post-capillary venules in vivo. *Biorheology* 44(5-6): 375–386.

LaMack J A, Friedman M H (2007) Individual and combined effects of shear stress

magnitude and spatial gradient on endothelial cell gene expression. *American Journal of Physiology Heart and Circulatoty Physiolgy* 293(5): H2853–H2859.

Lee D H, Kim N R, Lim B-S, Lee Y-K, Yang H-C (2009) Effects of TEGDMA and HEMA on the expression of COX-2 and iNOS in cultured murine macrophage cells. *Dental Materials* 25(2): 240–246.

Lee M-Y, Yoon H-W, Lee M-J, Kim K-M, Kwon J-S (2024). Thermophysical properties and bonding with composite resin of premixed mineral trioxide aggregate for use as base material. *Dental Materials Journal* 43(1): 58–66.

Lee W, Oh J-H, Park J-C, Shin H-I, Baek J-H, Ryoo H-M, et al. (2012) Performance of electrospun poly(ε-caprolactone) fiber meshes used with mineral trioxide aggregates in a pulp capping procedure. *Acta Biomaterialia* 8(8): 2986–2995.

Li J, Rao Z, Zhao Y, Xu Y, Chen L, Shen Z, et al. (2020) A decellularized matrix hydrogel derived from human dental pulp promotes dental pulp stem cell proliferation, migration, and induced multidirectional differentiation in vitro. *Journal of Endodontics* 46(10): 1438–1447.e5.

Li L, Terry C, Shiu Y-T, Cheung A (2008). Neointimal hyperplasia associated with synthetic hemodialysis grafts. *Kidney International* 74(10): 1247–1261

Luke A M, Patnaik R, Kuriadom S, Abu-Fanas S, Mathew S, Shetty K P (2020). Human dental pulp stem cells differentiation to neural cells, osteocytes and adipocytes an in vitro study. *Heliyon* 6(1): e03054.

Marˇsan T, Prpi´c-Mehicˇi´c G, Karlovi´c I, ˇSoˇstari´c B, Ani´c I, Karlovi´c Z (2003). Pulpal response to direct pulp capping with collagen bioresorbable membrane. *Acta Stomatologica Croatica* 37(1): 59-62.

Nakabayashi N, Takarada K (1992). Effect of HEMA on bonding to dentin. *Dental Materials* 8(2): 125–130

Patel S, Maria-Rios J, Parikh A, Okorie O N (2023). Diagnosis and management of elevated intracranial pressure in the emergency department. *International Jouranl of Emergency Medicine* 16(1): 72.

Seltzer S, Bender I B, Ziontz M (1963). The dynamics of pulp inflammation: correlations between diagnostic data and actual histologic findings in the pulp. *Oral Surgery. Oral Medicine. Oral Pathology. And Oral Radiology* 16: 846–871.

Sowmya N K, Tarun Kumar A B, Mehta D S (2010). Clinical evaluation of regenerative potential of type I collagen membrane along with xenogenic bone graft in the treatment of periodontal intrabony defects assessed with surgical re-entry and radiographic linear and densitometric analysis. *Journal of Indian Society of Periodontology* 14(1): 23–29.

Stenvik A, Iversen J, Mjör I (1972). Tissue pressure and histology of normal and inflamed tooth pulps in macaque monkeys *Archives of Oral Biology* 17(11): 1501–1511.

Reichl F X, Löhle J, Seiss M, Furche S, Shehata M M, Hickel R, et al. (2012). Elution of TEGDMA and HEMA from polymerized resin- based bonding systems. *Dental Materials* 28(11): 1120–1125.

Rodrigues N S, França C M, Tahayeri A, Ren Z, Saboia V P A, Smith A J, et al. (2021) Biomaterial and biofilm interactions with the pulp-dentin complex-on-a-chip *Journal of Dental Research* 100(10): 1136–1143.

Rowe A H, Pitt Ford T R (1990). The assessment of pulpal vitality. *International Endodontic Journal* 23(2): 77–83

Rutkowski J M, Swartz M A (2007). A driving force for change: interstitial flow as a morphoregulator. *Trends in Cell Biology* 17(1): 44–50

Vakis A, Koutentakis D, Karabetsos D, Kalostos G (2006). Use of polytetrafluoroethylene dural substitute as adhesion preventive material during craniectomies. *Clinical. Neurology and Neurosurgery* 108(8): 798–802.

Venzac B, Deng S, Mahmoud Z, Lenferink A, Costa A, Bray F, et al. (2021). PDMS curing inhibition on 3D-Printed molds: why? also, how to avoid it? *Analytical Chemistry* 93(19):

7180–7187.

Abstract in Korean

미세유체 흐름 장치를 활용한 경막 대체재의 생활치수치료 치수복조재로서의 적용 모델 구현

생활치수치료는 염증이 발생한 치수를 전체적으로 제거하는 대신 선택적으로 제거하여 치수의 생명력을 보존하는 보존적 치과 치료의 중요성이 증가함에 따라 주목받고 있다. 생활치수치료는 장기적인 추적관찰에서 높은 성공률을 보였지만, 일반적으로 사용되는 치수복조재인 Mineral trioxide aggregate (MTA) 에 의해 치근관이 석회화되는 부작용이 보고되었다. 치근관의 석회화는 재치료 시 기구의 접근을 어렵게 만드는 문제를 초래한다.

이 문제를 해결하기 위해 본 연구에서는 염증으로 인해 발생하는 치수 내 압력을 완화하도록 설계된 경막 대체재의 기계적 특성을 평가하고, 치수 내에서 중요한 역할을 하는 인간 치수 줄기세포 (hDPSC) 의 생물학적 반응을 조사했다. 또한 경막 대체재가 MTA 를 대체하는 치수복조재로 적용 가능한지 평가했으며, 이를 위해 치수 내 혈류 환경을 모사한 미세유체 흐름 장치 모델을 활용하였다. 또한, computational fluid dynamics (CFD) 시뮬레이션을 통해 미세유체 흐름 장치 내 유체 흐름 속도가 실제 치수 내 혈류 속도와 일치하도록 조정하였다.

더 나아가, 경막 대체재 (Biodesign 및 Neuro-patch) 는 상부 수복재 및 접착제로부터 방출되는 2-Hydroxypropyl Methacrylate (HEMA) 의 침투에 대한 저항성을 나타냈다. 따라서, 경막 대체재는 HEMA 침투 저항성을 바탕으로 생활치수치료의 유망한 대체 후보이다. 또한 미세유체 흐름 장치 모델은 실제

치수 조직에서 관찰되는 반응을 정밀하게 재현하였으며, 이는 향후 in vivo 테스트 플랫폼으로 활용될 가능성을 시사한다.

핵심 되는 말: 경막대체재, 인간 치수 줄기세포, 미세유체 흐름 장치, 생활치수치료